An Image Generator Platform to Improve Cell Tracking Algorithms
Simulation of Objects of Various Morphologies, Kinetics and Clustering

Pedro Canelas[1], Leonardo Martins[1], André Mora[1], Andre S. Ribeiro[2] and José Fonseca[1]
[1]*Computational Intelligence Group of CTS/UNINOVA, Faculdade de Ciências e Tecnologia, Universidade Nova de Lisboa, Quinta da Torre, 2829-516, Caparica, Portugal*
[2]*Laboratory of Biosystem Dynamics, Dep. of Signal Processing, Tampere University of Technology, Tampere, Finland*

Keywords: Microscopy, Synthetic Time-lapse Image Simulation, Cell Tracking, Cluster Tracking.

Abstract: Several major advances in Cell and Molecular Biology have been made possible by recent advances in live-cell microscopy imaging. To support these efforts, automated image analysis methods such as cell segmentation and tracking during a time-series analysis are needed. To this aim, one important step is the validation of such image processing methods. Ideally, the "ground truth" should be known, which is possible only by manually labelling images or in artificially produced images. To simulate artificial images, we have developed a platform for simulating biologically inspired objects, which generates bodies with various morphologies and kinetics and, that can aggregate to form clusters. Using this platform, we tested and compared four tracking algorithms: Simple Nearest-Neighbour (NN), NN with Morphology and two DBSCAN-based methods. We show that Simple NN works well for small object velocities, while the others perform better on higher velocities and when clustering occurs. Our new platform for generating new benchmark images to test image analysis algorithms is openly available at (http://griduni.uninova.pt/Clustergen/ClusterGen_v1.0.zip).

1 INTRODUCTION

Recent advances in live-cell microscopy imaging have enabled the acquisition of images with higher quality and resolution and the development of techniques for detecting and observing recently discovered cellular structures and their kinetics (Danuser, 2011; Sung and McNally, 2011).

The main challenges in live-cell imaging can be divided into two areas. The first relates to processes that occur before and during image acquisition in the microscope, associated with the refinement of processes, such as illumination, focus, drift correction, stage positioning and refinement of microscope components (e.g. shutter, lens, camera, stage) (Coutu and Schroeder, 2013). The second is related to post processing limitations, associated with storage of large amounts of data and image processing (e.g., image registration, segmentation, tracking, statistical quantification and background correction) (Coutu and Schroeder, 2013; Bonnet, 2004).

Automatic correction algorithms are normally included in microscope software packages (Frigault et al., 2009), while the process of image registration (overlaying two or more images of the same location taken at different time frames and/or from different viewpoints and/or by different sensorial devices) has been extensively studied and several methods are available. These are classified based on modality, intensity, type of data, dimensionality, domain and type of transformation, and registration methodologies (Deshmukh and Bhosle, 2011; Wyawahare et al., 2009).

The next step is related to the segmentation of cells or cellular structures of interest (Meijering 2012), where these segmented objects are detected, located, and separated from the background. The main challenge is to automatize this process and provide it with a high specificity and sensitivity for a vast number of cases. Presently, most algorithms are made available in open-source platforms and apply several approaches, such as intensity thresholding, feature detection, morphological filtering, region accumulation, deformable model fitting, etc. (Meijering, 2012).

When handling a time series, one needs to link the segmented objects in the actual frame with the ones from the previous frame, so as to extract the

Canelas, P., Martins, L., Mora, A., Ribeiro, A. and Fonseca, J.
An Image Generator Platform to Improve Cell Tracking Algorithms - Simulation of Objects of Various Morphologies, Kinetics and Clustering.
DOI: 10.5220/0005957800440055
In *Proceedings of the 6th International Conference on Simulation and Modeling Methodologies, Technologies and Applications (SIMULTECH 2016)*, pages 44-55
ISBN: 978-989-758-199-1

object's trajectory over time. Having available the information describing the target, defined by the state sequence X_k, $k \in \mathbb{N}$ (where $\mathbb{N}$ is the set of frames), and the measurements defined by Z_k, the objective of tracking is to estimate X_k, given all measurements until the moment $Z_{1:k}$ (Tissainayagam and Suter, 2005). This is made difficult by noise, occlusions, illumination changes, complex motions and object's shape dynamics, which can enhance the misidentification of object tracks over time (Yilmaz et al., 2006).

Presently available tools for segmentation and tracking in different microscopy settings include the 'Cell-C', based on DAPI staining and fluorescence *in situ* hybridization images (Selinummi et al., 2005), 'CellTracer', which applies morphological methods to automatically segment bacterial cells, yeast and human cells (Wang et al., 2010), 'MicrobeTracker' and its accessory tool 'SpotFinder', which segment *Escherichia coli* and *Caulobacter crescentus* cells and detected fluorescent spots within (Sliusarenko and Heinritz, 2011), 'Schnitzcells', which segments and tracks *E. coli* cells in confocal or phase contrast images (Young et al., 2012) and, 'CellAging', which was developed for cell segmentation and tracking in order to study the segregation and partitioning in cell division of protein aggregates (Häkkinen et al., 2013).

Validation of these image processing tools and techniques they use require the use of gold-standard images, usually manually annotated by biology experts. This is problematic, as it is expert-dependent (both inter-user and intra-user variability can be high) and are impractical in high-throughput data-sets (Coelho et al., 2009). To overcome this problem, a viable alternative is to generate artificial images using biologically inspired models. These images, whose ground truth is known, can be used for the accurate quantitative evaluation of image processing algorithms (Bonnet, 2004).

In Section 2, we give a comprehensive literature review of existing tools for simulation of synthetic microscopy images and the recent developments on cell tracking algorithms. In Section 3 we present the contributions to the development of the image simulation tool (models and parameters) and the implementation of three different tracking algorithms. In Section 4 the tracking results of several examples are presented using different parameters. Finally, in Section 5 we present final remarks on the development of the simulation tool and the results of the three algorithms, along potential future endeavours.

2 STATE OF THE ART

2.1 Synthetic Image Generators

There have been several contests and open challenges, usually requiring that each methodology is tested on the same benchmark data-sets (acquired by an independent laboratory or created by artificial image generators) (Meijering, 2012). Such artificial image generators require realistic biological models, and commonly use theoretical and experimental information regarding the statistical distributions of the object's behaviour (Xiong et al., 2010) but also spatial and temporal data from the object (Kruse, 2012; Misteli, 2007). If the object studied is a cell, these models should include morphology parameters such as cell shape and size, location of subcellular structures, kinetic and spatial statistics of cell growth, cell division, cell migration and models of internal cell functions.

The *modus operandi* of presently available tools to simulate microscopy images based on biological models can be divided in three stages: the digital phantom object generation, the simulation of the signal passing through the optical system and, the simulation of the image formed on a specific sensor (Svoboda et al., 2009).

Simulators such as 'SIMCEP' (Lehmussola et al., 2007) have provided a gold-standard platform to validate and test various image processing tools, such as the previously mentioned 'CellC' (Selinummi et al., 2005), the open-source and Java-based image processor ImageJ, and the commercially available MCID Analysis (Imaging Research Inc., Catharines, ON, Canada; Evaluation ver. 7.0), along with other image processing tools (Ruusuvuori et al., 2008). The phantom objects are generated with different cell parameters, such as probability of clustering, cell radius, and cell shape and with parameters related to the sensors and the optical system such as background noise and illumination disturbance (Ruusuvuori et al., 2008; Lehmussola et al., 2011).

Another toolbox, 'CytoPacq', was developed specifically to simulate all three phases, by being equipped with three different modules. The first module ('3D-cytogen') generates the digital object phantom, which imitates the cell structure and behaviour and can generate microspheres, granulocytes, HL-60 Nucleus and images of Colon Tissue. The second module ('3D-optigen') simulates the transmission of the signal through the lenses, objective, excitation filter and emission filter (various sets of equipment can be simulated). The last module, '3D-acquigen' is the digital CCD camera simulator of the phenomenons that occur during image capture (noise, sampling, digitization) by changing the camera selection, the acquisition time, the dynamic range usage and the stage z-step (Svoboda et al., 2007; Svoboda et al., 2009). The same group also introduced a novel versatile tool ('TRAgen'), capable of generating 2D time-lapses by simulating live cell populations as a ground-truth for the evaluation of cell tracking algorithms. They include models of cell motility, division and clustering up to tissue-level density (Ulman et al., 2015). Both simulators have been an important step in the simulation of cellular dynamics, such as measuring protein or RNA levels or even observing cell migration, division and growth (Coutu and Schroeder, 2013; Sung and McNally, 2011).

A recently developed toolbox called 'SimuCell' (Satwik et al., 2012) is capable of generating artificial microscopy images with heterogeneous cellular populations and diverse cell phenotypes. Each cell and their organelles are modelled with different shapes, having distinct distributions of biomarkers over each shape, which can be affected by the cell's microenvironment, showing the importance of good cell placement (*e.g.* in clusters, overlapping existing cells) (Satwik et al., 2012).

The 'CellOrganizer' toolbox was developed using a different approach, collecting laboratory data and using machine-learning techniques to generate the entire cell, including structures such as the nucleus, proteins, cell membrane and cytoplasm components (Murphy, 2012). Although the learn-based model was capable of extracting a very precise shape model, it could not be described it in precise mathematical terms (Zhao and Murphy, 2007).

Most image generators have focused on the simulation of morphological features and spatial information of the cell. Morphological information can suffice to create multidimensional images, but it cannot simulate time-lapsed multimodal and functional images, where important time-dependent processes are present. To simulate such images of bacterial cells, the 'miSimBa' (Microscopy Image Simulator of Bacterial Cells) tool has been under development (Martins et al., 2015). The simulated images can reproduce spatial and temporal bacterial time-dependent processes by modelling cell growth, division, motility and morphology: shape, size and spatial arrangement (Martins et al., 2015). Relevantly, these simulation tools can also be used to generate "null-models" (Gotelli and McGill, 1996) to study statistical patterns in absence of a particular mechanism (e.g. removing the nucleoid to study how it influences the spatial distribution of protein aggregates).

2.2 Cell Tracking

Several tracking methods have been proposed, differing mainly in how to process the available object features and on the type and number of tracked objects (Yilmaz et al., 2006). In order to decide which approach to follow, the object's representation, defined during the segmentation process, must be taken into account. Objects can be represented through points, geometric shapes, silhouette and contour, articulated shape model or skeletal model, leading to the development of different approaches (Yilmaz et al., 2006). In the same review, tracking methodologies were divided into three main categories: Point Tracking, Kernel Tracking and Silhouette Tracking. Objects in Point Tracking are represented by points and tracked based on their position and motion. The main issues of this methodology are the presence of occlusions and the entries and exits of objects from the field of view. This category has been split in Deterministic and Statistical methods. Deterministic methods associate each object with the application of motion constraints, while statistical methods take into account random perturbations and noise during the tracking process (Yilmaz et al., 2006). Nearest neighbour (NN) is the source of all deterministic approaches and uses only the distances between objects in k and k-1 matching the objects with the smallest distances. This distance can be based on position, shape, colour and size (Elfring et al., 2010).

An efficient visual object tracking algorithm was proposed by (Gu et al., 2011) that combines NN classification with descriptors based on the scale-invariant feature transform, efficient sub-window search and an updating and pruning method to achieve balance between stability and plasticity. This method successfully handles occlusions, clutter, and changes in scale and appearance.

The probabilistic data association filter (PDAF) and the joint probabilistic data association filter (JPDAF) are the basis for the statistical methods. PDAF uses a weighted average of the measurements as input, modelling only one target and considering linear dynamics and measurement models. JPDAF is an extension of PDAF, allowing multiple target tracking. The assumptions are the same, calculating the target's association probabilities jointly. In both methods, if the model is linear then the Kalman Filter has a relevant influence. One of the problems of these methods is the incapacity to recover from errors, because only the last measurement is used (Elfring et al., 2010). The Kalman filter is an optimal estimator, which means that it assumes parameters from indirect, inaccurate and uncertain observations and if all noise is Gaussian, the linear Kalman filter minimizes the mean square error of the estimated parameter. This filter is widely used to obtain the optimal state estimate (Elfring et al., 2010).

A different method (Gorji and Menhaj, 2007) combining the JDPAF and a particle filtering (Smith, 1993) was proposed and was named 'Monte Carlo JPDAF'. This method uses three models: the first with near constant velocity, the second with near constant acceleration and a third with both models, which achieved the best performance.

Another statistical method is the multiple hypothesis tracking (MHT), which is one of the most used with point features, but has computational limitations both in time and memory (Tissainayagam and Suter, 2005). This method postpones data association until enough information is available. The MHT starts by formulating all possible hypotheses, which develop into a set of new hypotheses each time new data arrives, generating a tree of hypothesis (Elfring et al., 2010). For each hypothesis, the position of the object in the next frame is predicted and then compared with the measurements, calculating their distance. The associations are made for each hypothesis, generating new hypotheses for the next iteration (Yilmaz et al., 2006). The tree of hypotheses should be cut, because it grows exponentially with the measured data. This can be done by clustering, i.e., measurements are subdivided into independent clusters. If a measurement cannot be associated with an existent cluster, a new one is created. Another way of cutting the tree is pruning, meaning that as new iterations are added, a part of the tree is deleted (Elfring et al., 2010).

Unlike PDAF and JPDAF, the MHT method can deal with objects entering, exiting and being occluded from the field of view. Kernel Tracking can be done using templates and density-based appearance models or multi-view appearance models. Templates use basic geometric shapes, while multi-view models encode different views of the object (Yilmaz et al., 2006). Mean shift and KLT (Kenade-Lucas-Tomasi) are examples of template and density-based appearance models.

In mean shift, the appearance of objects being tracked is defined by histograms. Similarities are measured using the Bhattacharyya coefficient (Bhattacharyya, 1943) and the Kullback-Leibler divergence (Joyce, 2014). The process tries to increase similarity between histograms, by repeating each iteration until they converge (Zhou et al., 2009).

KLT is an optical-flow method, which uses vectors to show the changes in the image (i.e. translation). A version of this method was proposed in which the translation of a region centred on an interest point is iteratively computed. Then, the tracker evaluates the tracked patch, computing a transformation between the corresponding patches in consecutive frames (Shi and Tomasi, 1994). These methods are effective while tracking single objects, but have problems dealing with multiple objects.

Silhouette Tracking consists in using precise information about the shape of the objects, using Shape Matching and searching for an object silhouette and its model in each frame. Each translation from frame to frame is handled separately by finding corresponding silhouettes detected in two consecutive frames. Another approach is based on the evolution of the object contour, connecting the correspondent objects by state space models or by minimizing the contour energy (Yilmaz et al., 2006). When tracking objects, one usually obtains multiple measurements and the incorrect ones are referred to as false measurements or clutter. The measurement with highest probability of being originated from the tracked object is then selected. If the algorithm selects the wrong measurement or if the correct measurement is not detected, a poor state is estimated. To solve this issue (reducing the computational cost), a validation region (measurement gate) is selected. The measurement gate is a region in which the next measurement has a higher emergence probability (Elfring et al., 2010).

3 METHODOLOGIES

3.1 Implementation of the Image Generator - Tool Interface and Basic Functionalities

The image generator interface and the tracking methods were implemented using the C# language from Visual Studio 2015. This sub-section focuses on the implementation of the image generator and the basic features. An intuitive and easy to understand interface was designed in order to facilitate the analysis of the tracking algorithms. The time-series generator allows the user to change a set of settings such as the number of objects, frames, clusters, and their features. The generator creates a csv file for each of the object's properties (position in x and y coordinates and a shape-related factor called "morphology", which is a rational number between 0 and 1). In this generator, objects are represented by circles and the morphology factor is assumed to be the radius. There is a conversion factor that determines the maximum radius of the objects (corresponding to morphology value 1). By default, this factor is initialized at 30. More factors and parameters can be added to the algorithm, increasing its complexity.

The tool interface is shown in Figure 1. At the top row of the window there are frame handlers, to advance forward and backward in the time-series, or to go directly to a specific frame. The "Time-Lapse" button reproduces the full time-series, one frame per 40 milliseconds.

The left bar contains the boxes to write the desired width and height of images, in pixels. Then the user can choose the number of objects in each frame, and the total number of frames. The "Maximum Velocity" is the maximum distance, in pixels, that an object can travel between frames, while the "Maximum Morphology Difference" is the maximum difference of the "morphology" factor that an object can have between frames, in percentage. The "Physical Move" button controls the option of giving objects physical limitations to their kinetics. If it is selected, each object has a velocity and orientation assigned to it, meaning that its position dynamics will depend on these two variables. If it is not selected, objects will move arbitrarily between frames.

One can also select "Allow Entries/Exits", to allow the objects to enter and exit the image limits. If unselected, objects collide with the edges of the image when reaching them.

Overlapping of cells is possible, using the "Allow Occlusions" option. When this option is selected, objects move without restrictions due to superposition between them. If it is not selected, objects will collide between them similarly as when colliding with the edges.

One can also force the objects to organize into clusters, by checking the "Create Clusters" option. When selected, all objects of each cluster have the same physical features. In this setting, "Physical Move" is automatically selected and "Allow Occlusions" is deselected, blocking the correspondent checkboxes. The button "Cluster Properties" (shown in Figure 2) leads to a new window with the options for clusters' creation. Here, one can choose the desired number of clusters, the number of objects per cluster, and the size of the clusters in pixels. It is also possible to choose between two types of objects' kinetics: "Follow the Leader" and "Alternative Movement". The application of "Cluster Centre Force" and its strength are shown in Figure 3 and explained in Section 3.2.2.

3.2 Object Modelling

This sub-section focuses on the modelled features,

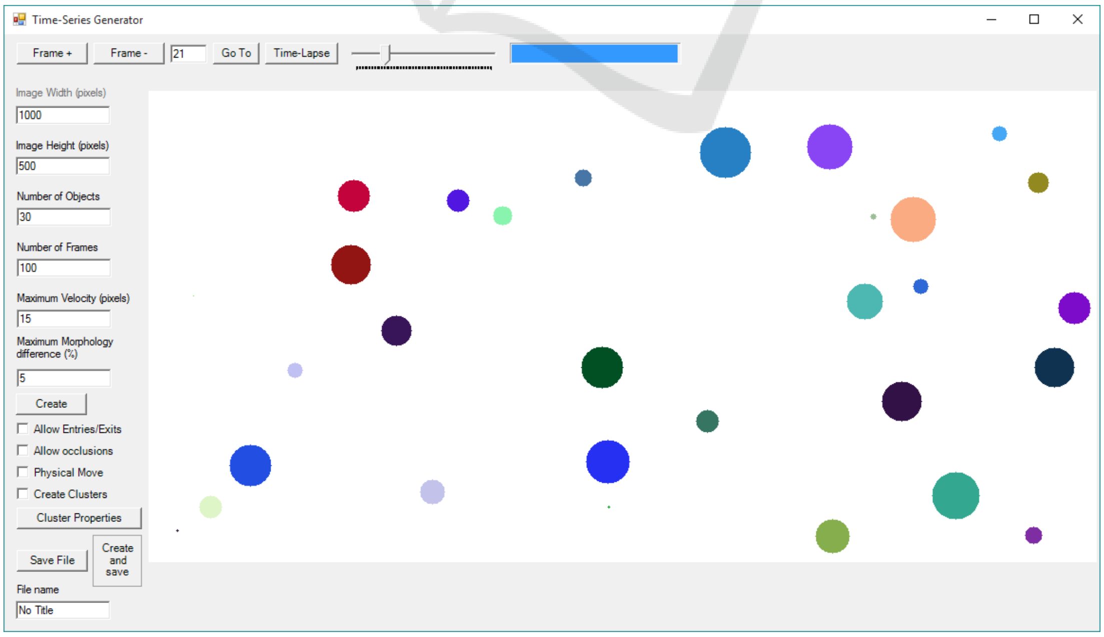

Frame: 21

Image Width (pixels): 1000

Image Height (pixels): 500

Number of Objects: 30

Number of Frames: 100

Maximum Velocity (pixels): 15

Maximum Morphology difference (%): 5

☐ Allow Entries/Exits

☐ Allow occlusions

☐ Physical Move

☐ Create Clusters

File name: No Title

Figure 1: Image Generator Tool interface.

namely object movement and cluster, based on biologically inspired objects, such as bacteria cells.

3.2.1 Object Motility

According to the user's selection, objects can have movement respecting a number of physical rules. If this option is deactivated, objects will move arbitrarily through the image.

Objects in each frame are only represented by their position in coordinates in x and y and their morphology factor. In each frame, each object can move to a new x and y coordinates by an arbitrary distance that cannot be higher than the "Maximum Velocity" value in pixels.

With occlusions and "exits and entries" also deactivated, objects will avoid the positions where they collide with other objects or go out the image boundaries, searching for a position considering these limitations and the maximum distance they can move between frames.

If the user chooses to give objects "Physical Move", in addition to previous features, each object will have a velocity and an orientation (physical parameters) assigned to it, meaning that their position dynamics will depend on these two values. In each frame, each object will have new x and y coordinates distanced "d" (no bigger than "Maximum Velocity") from the previous frame coordinates, direction "o" (between 0 and 2pi radians), with both components using an independent random variable.

If entries and exits are deactivated and if an object is heading to the image boundary, it is reflected respecting Snell's Law, causing a change in the angle's direction of movement. If occlusions are deactivated, when two objects are about to collide, they change to opposite orientations in an approximation to the reflection laws, but ignoring differences in their morphologies.

3.2.2 Cluster Creation

When selecting the option "Create Clusters", the Generator will create a time-series with the number of clusters, objects and size of cluster chosen by the user.

These options (shown in Figure 2) must be consistent and take into consideration the image size.

In "Alternative Movement" (as shown in Figure 3-A) all objects of each cluster have the same physical parameters, which means that they move in the same direction with the same speed (with a small independent arbitrary component).

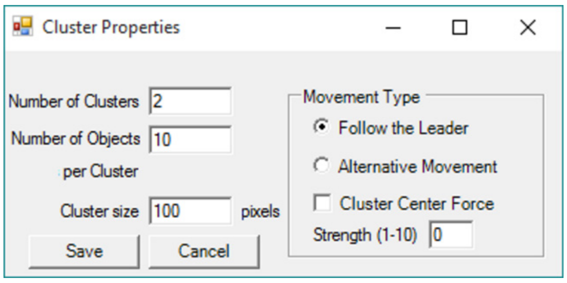
Cluster Properties

Number of Clusters: 2
Number of Objects per Cluster: 10
Cluster size: 100 pixels

Movement Type
[✓ Follow the Leader]
Alternative Movement
☐ Cluster Center Force
Strength (1-10): 0

Figure 2: Interface options for cluster properties.

In the "Follow the Leader" movement mode (as shown in Figure 3-B), each cluster has a leading object. The characteristics of the other objects of the same cluster are dependent on the leader's behaviour. The leader "receives" the physical parameters at first frame (velocity and orientation) and at each frame the other objects of its cluster will move in the leader's direction, minimizing the distance to it, but respecting the "non-collision" rule. If two objects from different clusters collide, one of them will start belonging to the other cluster. This may cause the "merging" of clusters.

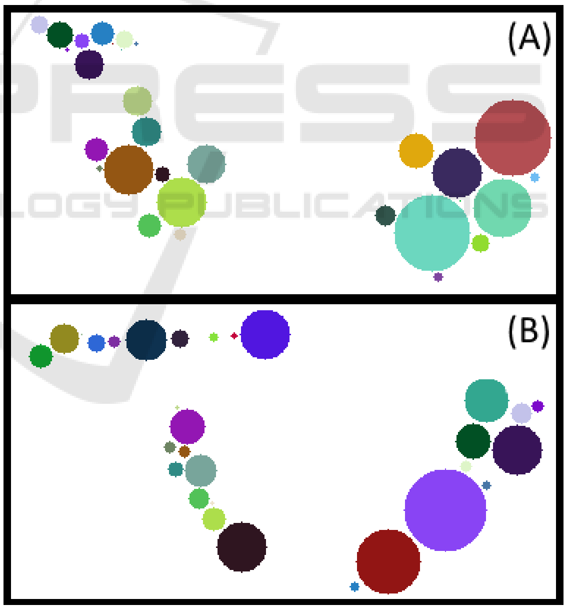

Figure 3: Exemplificative frames of (a) 'Alternative' Movement (b) 'Follow the leader' Movement.

The "Cluster Centre Force" feature is exclusively for "Alternative Movement" that creates an attraction force at the cluster's centre, with a selectable strength selected by the user. This force keeps cluster's objects together, even when colliding with the image borders or other objects. Increasing the strength, the objects will move faster to the cluster's centre. In this mode of motility, when objects from different clusters collide, they will be "left behind" by their cluster until they can join it again.

3.3 Tested Tracking Algorithms

3.3.1 Simple Nearest-Neighbour Algorithm

The first tracking algorithm tested was the Simple Nearest-Neighbour (NN). This method only takes into consideration the position of each object in each frame of the time-series, and uses the Euclidian Distance between points to find matching objects between frame *n* and *n+1*. Being d_p the distance between two objects:

$$d_p = \sqrt{(x_n - x_{n+1})^2 + (y_n - y_{n+1})^2} \quad (1)$$

Where x_n and y_n are the positions of each object in frame *n* and x_{n+1} and y_{n+1} are the positions in frame *n+1*. Having the distance between each object in frame *n* and all objects in frame *n+1*, correspondences are made based on the minimum distance. The object in frame *n+1* closer to each object in frame *n* is assigned to it. If two objects in *n+1* are assigned to the same object in *n*, the closer object is assigned, until all correspondences between frames are unique (Elfring et al., 2010).

3.3.2 Nearest-Neighbour with Morphology Algorithm

The next algorithm tested was the Nearest Neighbour with Morphology (NNm). This method accounts not only for the differences between the positions of each object in each frame, but also for a shape-related factor, called morphology.

This algorithm calculates the distance percolated by each object between frames *n* and *n+1* using equation (1). Being m_n the morphology of each object in frame *n,* and m_{n+1} the shape factor in *n+1*, the difference, d_m, between these variables is calculated by:

$$d_m = |m_n - m_{n+1}| \quad (2)$$

The total difference, d_t, between each object in each frame pair is given by (3) with α and β being the weights given to each partial distance.

$$d_t = \alpha \cdot d_p + \beta \cdot d_m \quad (3)$$

Here different weights are used (as presented in the Results section), in order to study the best way to combine them, to achieve the best possible results.

3.3.3 Cluster Tracking

Identifying clusters is one of the most complex issues of image characterization (Czink et al., 2006). In this work, the problem lays in tracking objects knowing that they are grouped in clusters. Bacteria often group in this way, so the goal is to find a method that improves tracking of clustered objects. One of the main problems of clustered objects is illustrated in Figure 4-A. Using Nearest-Neighbour (or Nearest Neighbour with Morphology) to track these frames, the algorithm will immediately misidentify at least two of the objects of frame *n+1*. This will occur in objects 1' and 3', and it happens because their position in *n+1* is exactly the same that objects 2 and 4 have in *n*.

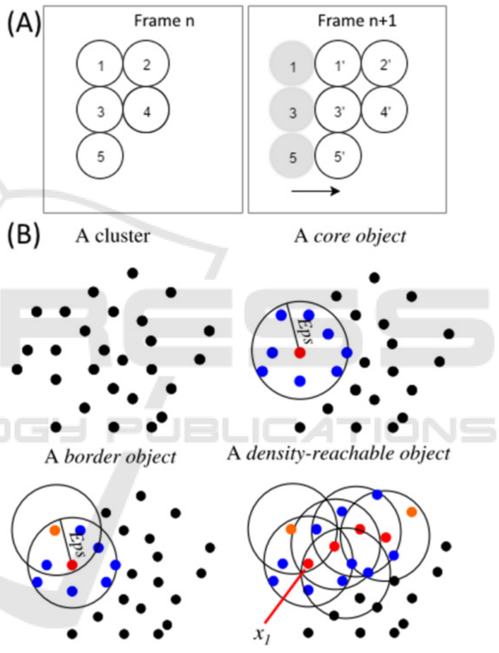

Figure 4: (A) Example of a possible misidentification using the Nearest-Neighbour Algorithms. (B) After defining 'MinPts' as the minimal number of objects in the neighbourhood, and Eps as the neighbourhood radius, we can define a core object (Red) when its local density is higher than 'MinPts' and a border object (Orange) if its local density is less than 'MinPts'. Two density-reachable objects are defined if there exists a chain of core objects with distances between them smaller than Eps. Adapted from (Tran et al., 2013).

To solve this problem we choose to implement a novel tracking algorithm that considers the cluster's features and singularities. The developed method to track clustered objects has several steps, and the first is to correctly identify the clusters and objects belonging to them. The method is called Density-

Based Spatial Clustering of Applications with Noise (DBSCAN) (Ester et al., 1996) in its revised version (Tran et al., 2013). This method formalizes the notion of "cluster" and "noise", using the definition of density to characterize clusters, which means that to define a cluster, the density of the neighbourhood of each point has to be higher than a given threshold. '*MinPts'* are the minimal number of objects in the neighbourhood, and *Eps* is the neighbourhood radius (see figure 4-B).

Objects can be divided in three categories: core, border and noise (see figure 4-B). An object is a core object if its local density is higher than '*MinPts'*. It is considered a border object if its local density is less than '*MinPts'* and it belongs to the neighbourhood of a core object. An object is classified as a noise if in its *Eps* radius there are less than '*MinPts'* objects and none is a core.

Finally, we identify two density-reachable objects if there exists a chain of core objects between them (see Figure 4-B), with distances between them smaller than '*MinPts'* (Tran et al., 2013).

This approach improves clustering identification when data has dense adjacent clusters (Tran et al.,, 2013). They also introduced the core-density-reachable objects, which are the same as the chain of density-reachable objects, but cutting border objects from chain's ends and staying unclassified until all core objects are identified (Tran et al., 2013).

The algorithm has two main steps: '*dbscan'* and '*ExpandCluster'*. The first step lies in covering each object and running '*ExpandCluster'* if the object is unclassified. Then, it returns all objects that are core-density-reachable from that one. If it is a core object, a cluster is produced. If it is a border object, it has no core-density-reachable objects, and follows to the next one. After all chains from the core object are known, it is assigned to its best density-reachable chain and all border objects.

After identifying the clusters in all frames with DBSCAN, a novel algorithm for object tracking was developed. This algorithm assumes that objects are grouped and move in clusters, treating each cluster as a separate individual while tracking. The first step (with all clusters identified) is to isolate the clusters and calculate their centroid, in coordinates x and y:

$$x_{centroid} = \sum_{i=1}^{N} x_i / N \tag{4}$$

After all centroids are calculated, they are processed as objects, since they have their own coordinates. The Nearest-Neighbour algorithm is then applied to these coordinates, tracking the clusters and resulting in a sequence of results similar to object tracking but treating a cluster individually.

4 RESULTS AND DISCUSSION

We generated several time-series that can be used as a benchmark to test tracking algorithms. For this, we simulated examples with different starting number of objects (20 to 160) and 'Maximum Velocity' (V=5, 10, 15, 20 and 30).

The generated images have a 1000x500 pixel size (first and second experiment) and 1500x100 (third experiment). The implemented Tracking Algorithms automatically processes the csv files with the objects' true positions produced by the Image Generator. The detected object tracking is then compared with the gold standard, where one error is counted when one object is incorrectly tracked from one frame to another it is considered a False Positive (FP). When one object is tracked correctly between two consecutive frames it is considered a True Positive (TP). It is important to notice that errors that occur in the beginning of the time series are typically propagated through the entire sequence. We present in the following tables the tracking errors (false discovery rate), calculated as FP/(FP+TP).

4.1 Simple Nearest-Neighbour Algorithm

We tested 10 time-series of 100 frames for each example with different objects and different maximum velocity. In Table 1, we present the tracking performance of the Simple Nearest-Neighbour Algorithm, based on the ground-truth produced by the image generator. A tracking error is calculated on every frame and accumulated to the end of the time-series.

Table 1: Tracking errors of the Simple Nearest-Neighbour Algorithm.

Obj.	V=5	V=10	V=15	V=20	V=30
20	0,00	0,92	1,06	4,19	19,20
40	0,26	1,27	3,23	5,93	24,01
60	0,06	1,58	5,63	12,38	39,66
80	0,24	1,84	6,62	15,74	45,06
100	0,27	1,20	7,85	19,94	49,76
120	0,22	1,69	10,57	21,16	51,86
140	0,55	3,71	14,16	26,57	58,07
160	0,42	4,12	14,91	33,74	63,89

In this case, the morphology shape-related factor called was set at 0.05 (this value was chosen to emulate biologically inspired objects that slowly change their shape over time).

The results from Table 1 show that this simple algorithm can still handle the increase in the number of objects while keeping a small velocity, and that increasing the velocity from 15 to 20 and 30 the tracking performance was significantly reduced.

4.2 Nearest-Neighbour with Morphology Algorithm

In this second experiment, we show how tracking taking into account the morphology of the object can be helpful in the worst case scenario of the last experiment. In Table 2, we present the results of the tracking performance of the Nearest-Neighbour with Morphology Algorithm.

In this case we also produced 10 time-series of 100 frames for each example with different objects and different maximum velocity, but also with distinct morphology factors.

We tested the algorithm in two configurations; the first giving a 60% importance to the calculated distance between objects (α factor in equation 3) and 40% to the calculated morphology difference (β factor). For the second configuration we used 40% for α and 60% for β. Here we also changed the shape-related factor and used both 0.05 and 0.1 values.

Table 2: Tracking errors of the Nearest-Neighbour with Morphology Algorithm.

	α = 60% and β=40%					
	m factor= 0.05			m factor= 0.1		
Obj.	V=15	V=20	V=30	V=15	V=20	V=30
100	6,02	14,71	41,60	6,03	17,79	40,55
120	6,27	14,92	42,05	9,24	19,68	44,45
140	9,29	18,34	48,96	8,34	21,59	48,90
160	10,32	25,49	55,35	10,26	25,39	55,32
Obj.	α = 40% and β=60%					
100	4,26	10,57	33,37	3,96	12,07	32,44
120	4,53	10,80	33,95	6,39	14,07	37,09
140	6,36	14,58	39,30	5,34	15,18	41,36
160	7,27	20,78	46,81	8,06	18,93	49,38

From Table 2, we observe that tracking results can be improved by using the Morphology Algorithm (e.g. in the worst case scenario the error percentage was reduced from 64% to 47%).

4.3 Cluster Tracking

The Create Clusters property was used to test the same tracking algorithms (Simple NN and NN with Morphology Algorithms with α = 40%). The simulated parameters were: number of clusters (1, 5 or 10), number of objects per cluster (10 or 15), maximum velocity (5 or 10), Alternative Movement, Center Force (4) and morphology factor (0 or 0.05). The tracking results are presented in table 3.

Table 3: Tracking errors, within clusters with different properties, using the Simple and Morphology Nearest-Neighbour Algorithms.

		Simple NN Algorithm			
Nº of Clust	Obj. / Clust.	m factor= 0		m factor= 0.05	
		V=5	V=10	V=5	V=10
1	10	7,79	30,42	9,88	23,33
1	15	11,74	50,91	10,74	38,06
5	10	7,48	34,71	10,95	31,89
5	15	17,43	45,22	16,06	44,51
10	10	12,20	38,26	11,64	42,47
10	15	21,14	53,90	23,52	57,34
		NN with Morphology			
1	10	1,27	4,879	5,52	13,83
1	15	3,76	21,15	4,63	20,76
5	10	1,80	12,98	4,69	15,93
5	15	7,16	20,77	5,94	22,07
10	10	3,78	16,15	4,55	19,71
10	15	8,73	28,36	10,13	34,12

For the Cluster creation, we used 10 time-series (and averaged the results) of 200 frames and calculated the object tracking on every frame and accumulated to the end of the time-series.

The DBSCAN algorithm tries to separate each cluster in every frame. Therefore, if the number of clusters is the same between the actual frame and the previous one (t and t-1), then they are matched using NN, treating them as isolated objects and aligned using their centroids. If the number of clusters changes, we skip the first step and check the number of objects inside each cluster. When there are more objects in t then in t-1, these 'extra' objects are called 'Possible Entry', if there are less objects, they are called 'Possible Exit'.

This classification is done temporarily and compares the "Possible Exit" features to the features of all other objects of the frame t-1, linking it to a "Possible entry" in another cluster (meaning that it left one cluster to join another), classifying it as noise, or as an object leaving the image. The main difference between the two DBSCAN Algorithms is that, in the first, this classification is done after the tracking and in the second it is done before the tracking, equalizing the number of objects between the clusters.

Results from both DBSCAN Algorithms are presented in Table 4. We can see that DBSCAN Algorithms do not improve significantly over the Nearest-Neighbour with Morphology.

Table 4: Tracking errors, within clusters with different properties, using two different DBSCAN Algorithms.

		DBSCAN 1			
Nº of Clust	Obj. / Clust.	m factor= 0		m factor= 0.05	
		V=5	V=10	V=5	V=10
1	10	5,55	2,97	9,64	9,14
1	15	1,92	12,94	3,87	10,49
5	10	5,43	13,71	6,42	16,61
5	15	5,84	19,29	6,49	20,84
10	10	5,81	17,55	6,42	21,07
10	15	8,65	28,29	9,91	34,52
		DBSCAN 2			
1	10	4,67	2,97	9,64	7,82
1	15	2,59	12,96	3,87	10,49
5	10	5,54	14,56	7,55	17,37
5	15	5,74	19,35	6,19	20,82
10	10	6,00	17,57	6,43	21,42
10	15	8,65	28,29	9,98	34,52

A strange behaviour with just 1 cluster was identified in the DBSCAN algorithms, where increasing the objects actually decreased the tracking errors. This behaviour could be due to a bigger movement restriction within clusters with higher objects, but further studies are required to analyse this behaviour.

5 CONCLUSIONS AND FUTURE WORK

To support high-throughput experiments of single cell imaging, reliable automated image processing methods are required. Although most studies focus on automatic segmentation of cells or cellular structures, in a time-series a proper object tracking is also necessary, particularly since errors in tracking are propagated, meaning that even small tracking errors (particularly on the initial frames) can lead to a high percentage of misidentified tracks.

To validate such Tracking Algorithms, it is necessary to use a labelled ‘ground truth’. Sometimes this ground-truth is manually processed, which can be unfeasible in a Big Data scenario. A more viable alternative is to generate artificial images by simulating biological cell models. To produce such artificial images we developed an open source platform that can simulate biologically inspired bacterial systems, by creating cells with different morphologies, physical movement and cluster creation. Using this Platform, we evaluated three tracking algorithms (Simple Nearest-Neighbour, Nearest-Neighbour with Morphology and two variations of the DBSCAN Algorithm).

The obtained results showed that, for cases with lower maximum velocity, the Simple Nearest-Neighbour Algorithm was able to track objects even with a significant increase in the number of objects. The Nearest-Neighbour with Morphology algorithm can help in reducing tracking errors when the velocity is increased. In the example where we forced the creation of clusters, both the Nearest-Neighbour with Morphology and the DBSCAN algorithms showed similar results. In the near future, we plan to study and compare other tracking methodologies in different cluster configurations.

We expect this open-sourced tool (available at: http://griduni.uninova.pt/Clustergen/ClusterGen_v1.0.zip) to help future endeavours in the development of new tracking algorithms, as it can produce huge amount of benchmarked data in various configurations.

Future developments of this tool involve adding an object division module, which can be used to test division tracking in dense clusters. We also plan to add a module that introduces secondary bodies inside the primary objects, simulating internal cell organelles and structures. A future application will also be made available as a web-based system to improve usability and compatibility.

ACKNOWLEGMENTS

Work supported by the Portuguese Foundation for Science and Technology (FCT/MCTES) through a PhD Scholarship, ref. SFRH/BD/88987/2012 to LM, SADAC project (ref. PTDC/BBB-MET/1084/2012) and by FCT Strategic Program UID/EEA/00066/203 of UNINOVA, CTS. This work is also funded by the Academy of Finland [ref. 126803 to ASR].

REFERENCES

Bhattacharyya, A., 1943. On a Measure of Divergence Between Two Statistical Populations Defined by Probability Distributions. *Bulletin of the Calcutta Mathematical Society*, 35, pp.99–110.

Bonnet, N., 2004. Some trends in microscope image processing. *Micron (Oxford, England : 1993)*, 35(8), pp.635–653.

Coelho, L.P., Shariff, A. & Murphy, R.F., 2009. Nuclear Segmentation In Microscope Cell Images A Hand-Segmented Dataset And Comparison Of Algorithms. In *Proc IEEE Int Symp Biomed Imaging*. pp. 518–521.

Coutu, D.L. & Schroeder, T., 2013. Probing cellular processes by long-term live imaging--historic problems and current solutions. *Journal of cell science*, 126(Pt 17), pp.3805–15.

Czink, N., Mecklenbräuker, C. & Del Galdo, G., 2006. A novel automatic cluster tracking algorithm. *IEEE International Symposium on Personal, Indoor and Mobile Radio Communications, PIMRC*, pp.1–5.

Danuser, G., 2011. Computer vision in cell biology. *Cell*, 147(5), pp.973–8.

Deshmukh, M. & Bhosle, U., 2011. A survey of image registration. *International Journal of Image Processing*, 5(3), pp.245–269.

Elfring, J., Janssen, R. & van de Molengraft, R., 2010. Data Association and Tracking: A Literature Survey. In *ICT Call 4 RoboEarth Project.*

Ester, M. et al., 1996. A Density-Based Algorithm for Discovering Clusters in Large Spatial Databases with Noise. In *2nd Int. Conference on Knowledge Discovery and Data Mining*. pp. 226–231.

Frigault, M. et al., 2009. Live-cell microscopy - tips and tools. *Journal of Cell Science*, 122(6), pp.753–767.

Gorji, A. & Menhaj, M.B., 2007. Multiple Target Tracking for Mobile Robots Using the JPDAF Algorithm. In *19th IEEE International Conference on Tools with Artificial Intelligence (ICTAI 2007)*. pp. 137–145.

Gotelli, N.J. & McGill, B.J., 1996. Null versus neutral models: what's the difference? *Ecography*, 29(5), pp.793–800.

Gu, S., Zheng, Y. & Tomasi, C., 2011. Efficient visual object tracking with online nearest neighbor classifier. In *Computer Vision – ACCV 2010. Volume 6492 of the series LNCS*. pp. 271–282.

Häkkinen, A. et al., 2013. CellAging: a tool to study segregation and partitioning in division in cell lineages of Escherichia coli. *Bioinformatics (Oxford, England)*, 29(13), pp.1708–1709.

Joyce, J., 2014. Kullback-Leibler Divergence. In M. Lovric, ed. *International Encyclopedia of Statistical Science SE - 327*. Springer Berlin Heidelberg, pp. 720–722.

Kruse, K., 2012. Bacterial Organization in Space and Time. In *Comprehensive Biophysics*. pp. 208–221.

Lehmussola, A. et al., 2007. Computational framework for simulating fluorescence microscope images with cell populations. *IEEE transactions on medical imaging*, 26(7), pp.1010–6.

Lehmussola, A. et al., 2011. Synthetic Images of High-Throughput Microscopy for Validation of Image Analysis Methods. *Proceedings of the IEEE*, 96(8), pp.1348 – 1360.

Martins, L., Fonseca, J. & Ribeiro, A., 2015. "miSimBa" - A simulator of synthetic time-lapsed microscopy images of bacterial cells. In *Proceedings - 2015 IEEE 4th Portuguese Meeting on Bioengineering, ENBENG 2015*. pp. 1 – 6.

Meijering, E., 2012. Cell Segmentation: 50 Years Down the Road. *IEEE Signal Processing Magazine*, 29(5), pp.140–145.

Misteli, T., 2007. Beyond the sequence: cellular organization of genome function. *Cell*, 128(4), pp.787–800.

Murphy, R., 2012. CellOrganizer: Image-derived Models of Subcellular Organization and Protein Distribution. *Methods in Cell Biology*, 110, pp.179–93.

Ruusuvuori, P. et al., 2008. Benchmark Set Of Synthetic Images For Validating Cell Image Analysis Algorithms. In *Proceedings of the 16th European Signal Processing Conference, EUSIPCO.*

Satwik, R. et al., 2012. SimuCell : a flexible framework for creating synthetic microscopy images a PhenoRipper : software for rapidly profiling microscopy images. , 9(7), pp.634–636.

Selinummi, J. et al., 2005. Software for quantification of labeled bacteria from digital microscope images by automated image analysis. *BioTechniques*, 39(6), pp.859–863.

Shi, J. & Tomasi, C., 1994. Good features to track. In *Proceedings CVPR'94. 1994 IEEE Computer Society Conference on. IEEE*. pp. 593–600.

Sliusarenko, O. & Heinritz, J., 2011. High-throughput, subpixel precision analysis of bacterial morphogenesis and intracellular spatio-temporal dynamics. *Molecular Microbiology*, 80(3), pp.612–627.

Smith, A., 1993. Novel approach to nonlinear/non-Gaussian Bayesian state estimation. *Radar and Signal Processing, IEE Proceedings F*, 140(2), pp.107–113.

Sung, M.-H. & McNally, J.G., 2011. Live cell imaging and systems biology. *Wiley interdisciplinary reviews. Systems biology and medicine*, 3(2), pp.167–82.

Svoboda, D. et al., 2007. On simulating 3D Fluorescent Microscope Images. In *Computer Analysis of Images and Patterns -12th International Conference, CAIP 2007, Vienna, Austria, August 27-29, 2007. Proceedings*. pp. 309–316.

Svoboda, D., Kozubek, M. & Stejskal, S., 2009. Generation of digital phantoms of cell nuclei and simulation of image formation in 3D image cytometry. *Cytometry. Part A : the journal of the International Society for Analytical Cytology*, 75(6), pp.494–509.

Tissainayagam, P. & Suter, D., 2005. Object tracking in image sequences using point features. *Pattern Recognition*, 38(1), pp.105–113.

Tran, T.N., Drab, K. & Daszykowski, M., 2013. Revised DBSCAN algorithm to cluster data with dense adjacent clusters. *Chemometrics and Intelligent Laboratory Systems*, 120, pp.92–96.

Ulman, V., Oremus, Z. & Svoboda, D., 2015. TRAgen: A Tool for Generation of Synthetic Time-Lapse Image Sequences of Living Cells. In *Proceedings of 18th International Conference on Image Analysis and Processing (ICIAP 2015)*. Springer International Publishing, pp. 623–634.

Wang, Q. et al., 2010. Image segmentation and dynamic lineage analysis in single-cell fluorescence microscopy. *Cytometry A*, 77(1), pp.101–110.

Wyawahare, M., Patil, P. & Abhyankar, H., 2009. Image Registration Techniques : An overview. *Int. Journal of Signal Processing, Image Processing and Pattern Recognition*, 2(3), pp.11–28.

Xiong, W. et al., 2010. Learning Cell Geometry Models For Cell Image Simulation : An Unbiased Approach. In *Proceedings of 2010 IEEE 17th International Conference on Image Processing*. pp. 1897–1900.

Yilmaz, A., Javed, O. & Shah, M., 2006. Object tracking: A survey. *ACM Computing Surveys*, 38(4, Article 13), pp.1–45.

Young, J. et al., 2012. Measuring single-cell gene expression dynamics in bacteria using fluorescence time-lapse microscopy. *Nat. Protoc.*, 7(1), pp.80–8.

Zhao, T. & Murphy, R.F., 2007. Automated learning of generative models for subcellular location: building blocks for systems biology. *Cytometry. Part A : the journal of the International Society for Analytical Cytology*, 71(12), pp.978–90.

Zhou, H., Yuan, Y. & Shi, C., 2009. Object tracking using SIFT features and mean shift. *Computer Vision and Image Understanding*, 113(3), pp.345–352.